

Geologic carbon cycle constraints on the terrestrial hydrological response to higher atmospheric CO₂

Jeremy K. C. Rugenstein^{1,2} and Alexander J. Winkler^{2,3}

¹Department of Geosciences, Colorado State University, Fort Collins, CO, USA

²Max Planck Institute for Meteorology, Hamburg, Germany

³Max Planck Institute for Biogeochemistry, Jena, Germany

Contents of this file

Text S1

Figures S1 to S2

Tables S1 to S2

Introduction

This supplementary file contains a detailed description of the model equations used in CH₂O-CHOO and their derivation. It also contains several figures relevant to understanding the arguments in the main text as well as tables that contain model parameters, both for CH₂O-CHOO and for the Earth system models that were investigated for their runoff sensitivity.

Text S1. Model Framework

We modify a carbon cycle model to incorporate runoff (q) into the equations that predict carbon mass balance. CH₂O-CHOO is adapted from and is a simplified version of CLiBeSO-W (Caves Rugenstein et al., 2019), which is itself based upon aspects of the COPSE and GEOCARB models (Berner, 2006; Lenton et al., 2018; Shields and Mills, 2017). The mass balance forward model solves for the time-varying reservoirs of carbon (C) and alkalinity (A) as a function of the major fluxes of C and A to and from the ocean-atmosphere, according to equations 1 and 2:

$$\frac{dC}{dt} = F_{carb w} + F_{org w} + F_{volc} - F_{carb b} - F_{org b} \quad (1),$$

and

$$\frac{dA}{dt} = 2F_{carb\omega} + 2F_{sil\omega} - 2F_{carb\beta} \quad (2),$$

where $F_{carb\omega}$, $F_{org\omega}$, and $F_{sil\omega}$ are the carbonate, organic, and silicate weathering fluxes, F_{volc} is the volcanic flux, and $F_{carb\beta}$ and $F_{org\beta}$ are the carbonate and organic burial fluxes [mol C/yr].

We treat $F_{sil\omega}$ as a function of q and the concentration of silicate-weathering derived bicarbonate ($[C]_{sil}$):

$$F_{sil\omega} = F_{sil\omega,0} \times R_q \times R_{[c]} \quad (3),$$

where $F_{sil\omega,0}$ is the initial, pre-perturbation weathering flux, R_q is the ratio of q at time t to initial q (q_0), and $R_{[c]}$ is the ratio of $[C]_{sil}$ at time t to the initial $[C]_{sil}$ ($[C]_{sil,0}$). We calculate q as an exponential function of global temperature (T [K]), which is itself logarithmically related to atmospheric CO_2 (Knutti et al., 2017; Myhre et al., 1998):

$$q = q_0(1 + \lambda_q)^{\Delta T} \quad (4),$$

where λ_q describes the sensitivity of q to T [%/K] (*i.e.*, the q -sensitivity), and ΔT is calculated via its relationship to climate sensitivity:

$$\Delta T = S_{eq} \log_2(R_{CO_2}) \quad (5),$$

where S_{eq} is the equilibrium climate sensitivity and R_{CO_2} is the ratio of atmospheric CO_2 at time t ($CO_{2,t}$) and the pre-perturbation CO_2 ($CO_{2,0}$).

The value of $[C]_{sil}$ is calculated using modified equations from Maher and Chamberlain (2014) (*i.e.*, the MAC model, following derivations in Graham and Pierrehumbert (2020)). These equations permit us to explicitly incorporate the effect of T , q , and weathering zone pCO_2 —all sensitive to atmospheric CO_2 and climate—on $[C]_{sil}$.

$$[C]_{sil} = [C]_{sil,eq} \left(\frac{\frac{Dw}{q}}{1 + \frac{Dw}{q}} \right) \quad (6),$$

where $[C]_{sil,eq}$ is the maximum, equilibrium concentration of silicate-derived bicarbonate and Dw is the Damköhler weathering coefficient, which is a term that encapsulates the reactivity of the weathering zone and time required to reach equilibrium. Following Maher and Chamberlain (2014), we define Dw as:

$$Dw = \frac{L_\phi r_{max} \frac{1}{1 + Ts \times r_{eff}}}{[C]_{sil,eq}} \quad (7),$$

where L_ϕ is the reactive length scale (held constant for our simulations), r_{max} is the theoretical maximum reaction rate (held constant for our simulations), Ts is the age of the weathering zone and is a key variable describing the reactivity of the weathering zone, and r_{eff} is the effective reaction rate. This effective reaction rate is defined as:

$$r_{eff} = ke^{\left[\frac{Ea}{Rg}\left(\frac{1}{T} - \frac{1}{T_0}\right)\right]} \quad (8),$$

where R_g is the universal gas constant [J/K/mol], Ea is the activation energy [J/mol], and the exponential term is an Arrhenius function to describe the effect of T on reaction rates (Brady, 1991; Kump et al., 2000). The coefficient k [y^{-1}] encapsulates the effects of mineral surface area, molar mass, and the reference reaction rate (all assumed constant) that modulate the effect of T on r_{eff} .

Lastly, $[C]_{sil,eq}$ is modified by the availability of reactant, which here is assumed to be dominantly CO_2 . We calculate this effect as a function of weathering zone pCO_2 assuming open-system CO_2 dynamics, following Winnick and Maher (2018):

$$[C]_{sil,eq} = [C]_{sil,eq,0} (R_{CO_2,wz})^{0.316} \quad (9),$$

where $[C]_{sil,eq,0}$ is the pre-perturbation, initial value of $[C]_{sil,eq}$. $R_{CO_2,wz}$ is the ratio of weathering zone pCO_2 at time t (WZ_{CO_2}) to the initial weathering zone pCO_2 pre-perturbation ($WZ_{CO_2,0}$). We calculate $R_{CO_2,wz}$ using a formulation proposed by Volk (1987) that links weathering zone pCO_2 with the primary source of that CO_2 , which is aboveground terrestrial gross primary productivity (GPP). Here, WZ_{CO_2} is calculated using an equation that links GPP , CO_2 fertilization on GPP , and weathering zone CO_2 :

$$WZ_{CO_2} = \left[R_{GPP} \left(1 - \frac{CO_{2,0}}{WZ_{CO_2,0}} \right) + \frac{CO_2}{WZ_{CO_2,0}} \right] WZ_{CO_2,0} + (CO_2 - CO_{2,0}) \quad (10).$$

Here, R_{GPP} is the ratio of GPP at time t to the pre-perturbation GPP (GPP_0) and the last term on the right-hand side of the equation ensures that WZ_{CO_2} is always greater than atmospheric CO_2 . GPP is calculated using a Michaelis-Menton formulation, following Volk (1987):

$$GPP = GPP_{max} \left[\frac{CO_2 - CO_{2,min}}{CO_{2,half} + (CO_2 - CO_{2,min})} \right] \quad (11),$$

where GPP_{max} is the maximum possible global terrestrial GPP , $CO_{2,min}$ is the CO_2 at which photosynthesis is balanced exactly by photorespiration, and $CO_{2,half}$ is the CO_2 at which GPP is equivalent to 50% GPP_{max} :

$$CO_{2,half} = \left(\frac{GPP_{max}}{GPP_0} - 1 \right) (CO_{2,0} - CO_{2,min}) \quad (12).$$

We choose a $CO_{2,min}$ of 100 ppm based upon evidence for widespread CO_2 starvation at the Last Glacial Maximum (LGM) (Prentice and Harrison, 2009; Scheff et al., 2017), which had an atmospheric CO_2 of ~ 180 ppm. We also assume that GPP_{max} is equal to twice GPP_0 , though our results are insensitive to this parameter. Lastly, we assume that $WZ_{CO_2,0}$ is 10x larger than $pCO_{2,0}$ given evidence that soil CO_2 is typically elevated above atmospheric levels by approximately an order of magnitude (Brook et al., 1983).

Figure S1. The percentage change in $[C]_{\text{sil}}$ as atmospheric CO_2 doubles as a function of the q -sensitivity, using the Maher and Chamberlain (2014) formulation of weathering. Generally, $[C]_{\text{sil}}$ increases even if q increases, unless q increases are so large (8-16 %/K) that increasing q causes dilution that overwhelms the effect from rising temperatures and increasing soil $p\text{CO}_2$. However, changes in $[C]_{\text{sil}}$ are less than 1:1 with changes in q , as indicated by the lower slope of the black lines relative to the 1:1 line (red). Solid line uses the standard parameters (Table S1); dashed line assumes an $8^\circ \text{K}/\text{CO}_2$ doubling equilibrium climate sensitivity; dot-dashed line assumes that soil $p\text{CO}_2$ scales 1:1 with atmospheric $p\text{CO}_2$ (rather than using the Volk (1987) formulation that relates soil $p\text{CO}_2$ to atmospheric $p\text{CO}_2$); long dashed line uses a higher activation energy ($E_a = 76 \text{ kJ/mol}$).

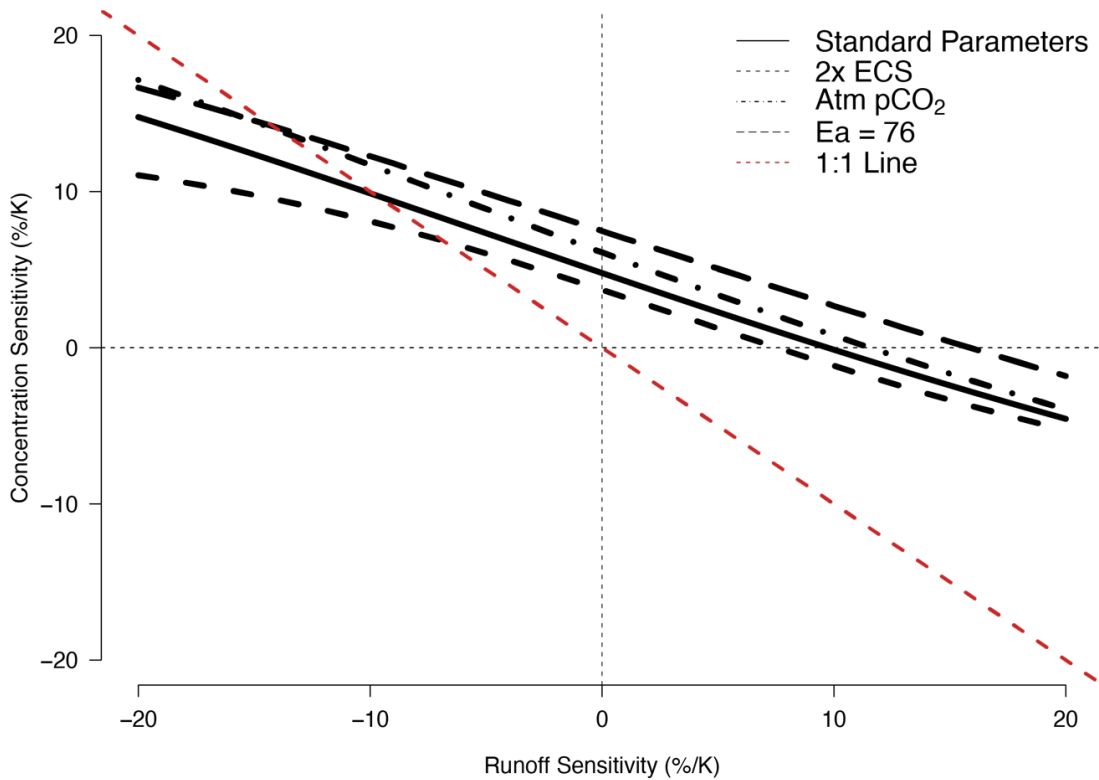


Figure S2. Effect of variations of weathering zone age (T_s) on the recovery time using the West (2012) formulation of weathering zone fluxes. Red line uses the standard values (Table S1) and the Maher and Chamberlain (2014) formulation of weathering fluxes. Gray vertical bar indicates the range of runoff sensitivity estimated using the C4MIP model ensemble (see main text).

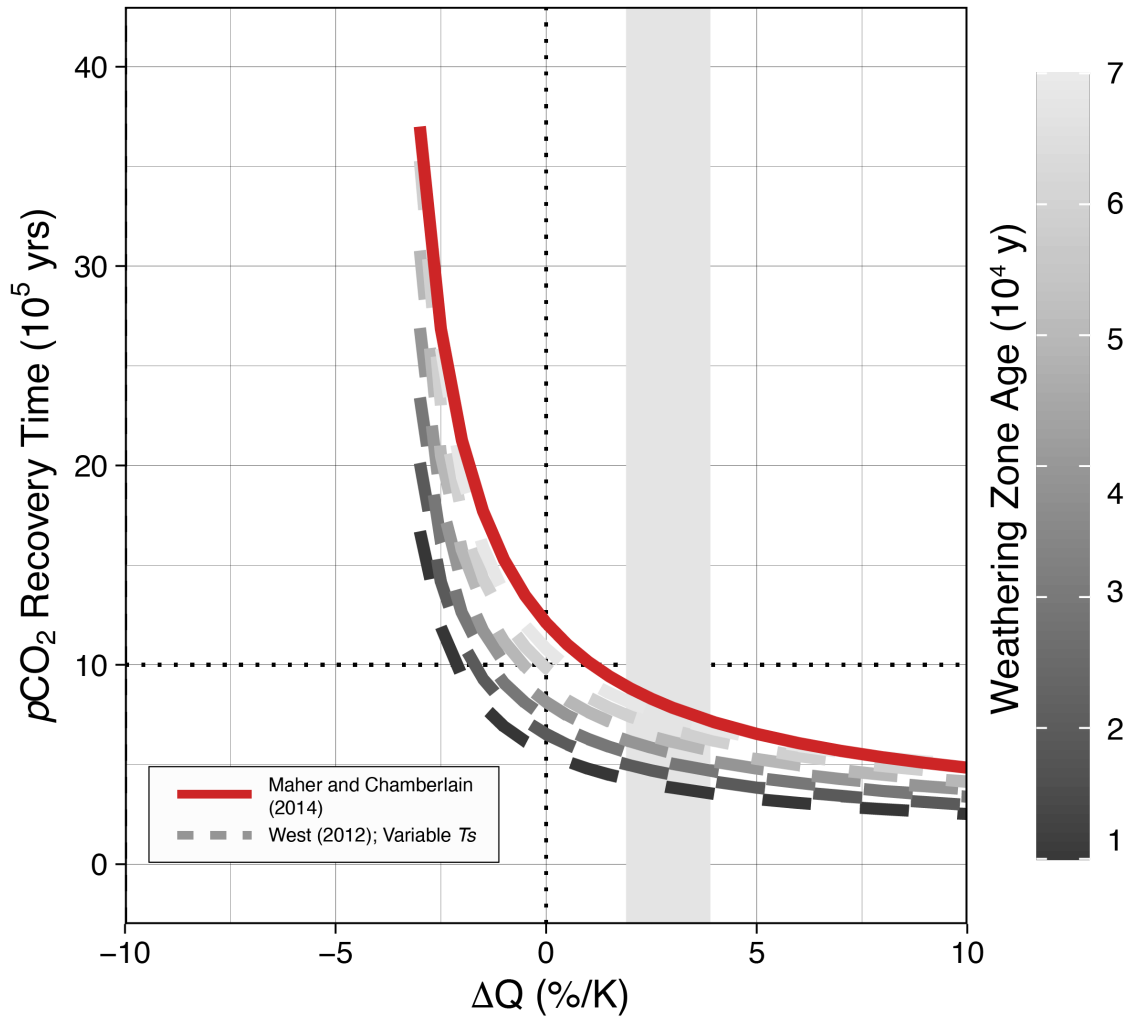


Table S1. Parameters used in the CH₂O-CHOO model, organized by model sub-component. Sources are listed if different from the original model formulation in Maher and Chamberlain (2014) or West (2012).

| Parameters | Optimized Values | Units | Source |
|---|------------------|---|-----------------------------|
| Climate parameters | | | |
| Earth System Sensitivity | 4 | K/CO ₂ doubling | Knutti et al. (2017) |
| Initial Earth Surface T | 15 | K | |
| q_0 | 0.3 | m/yr | Manabe et al. (2004) |
| $p\text{CO}_2$ | 400 | ppm | |
| pH | 8.15 | – | |
| Carbon cycle model parameters | | | |
| $F_{\text{silw},0}$ | 6 | 10 ¹² mol C/yr | Moon et al. (2014) |
| $F_{\text{carb},0}$ | 12 | 10 ¹² mol C/yr | Gaillardet et al. (1999) |
| $F_{\text{org},0}$ | 6 | 10 ¹² mol C/yr | Berner (2006) |
| $F_{\text{carb},0}$ | 18 | 10 ¹² mol C/yr | Milliman and Droxler (1996) |
| $F_{\text{org},0}$ | 6 | 10 ¹² mol C/yr | |
| $F_{\text{volc},0}$ | 6 | 10 ¹² mol C/yr | Wallmann (2001) |
| Maher and Chamberlain (2014) model parameters | | | |
| r_{eff} | 8.7 | 10 ⁻⁶ mol/m ² /yr | |
| m | 270 | g/mol | |
| A | 0.1 | m ² /g | |
| r_{max} | 1085 | μmol/L/yr | |
| L_{ϕ} | 0.1 | m | |
| T_S | 2 | 10 ⁴ yr | Larsen et al. (2014) |
| C_{eq} | 374 | μmol/L | |
| E_a | 38 | kJ/mol | |
| West (2012) model parameters | | | |
| K | 2.6 | 10 ⁻⁴ | |
| K_w | 7.6 | 10 ⁻⁵ | |
| z | 8.9 | – | |
| X_m | 0.09 | – | |
| σ | 0.89 | – | |

Table S2. Overview of CMIP5/6 models included in this study (Arora et al., 2020, 2013)

| Models | MPI-ESM1-2-LR | UKESM1-0-LL | CNRM-ESM2-1 | IPSL-CM6A-LR | ACCESS-ESM1-5 | NorESM1-ME | CESM1-BGC | IPSL-CM5A-LR |
|--------------------|---------------|----------------|-------------|----------------------|------------------------|-------------|-------------|--------------|
| Generation | CMIP6 | CMIP6 | CMIP6 | CMIP6 | CMIP6 | CMIP5 | CMIP5 | CMIP5 |
| No. of PFTs | 13 | 13 | 16 | 15 | 13 | 16 | 16 | 5 |
| Land Model | JSBACH3.2 | JULES-ES-1.0 | ISBA-CTRIP | ORCHIDEE, branch 2.0 | CABLE2.4 with CASA-CNP | CLM4 | CLM4 | ORCHIDEE |
| Land resolution | 1.8° x 1.8° | 1.875° x 1.25° | 1.4° x 1.4° | 2.5° x 1.3° | 1.875° x 1.25° | 2.5° x 1.9° | 0.9° x 1.2° | 2° x 0.5°—2° |
| Dynamic vegetation | Yes | Yes | No | No | No | No | No | No |
| Nitrogen cycle | Yes | Yes | No | No | Yes | Yes | Yes | No |
| Fire | Yes | No | Yes | No | No | Yes | Yes | Yes |